processes

MDPI

Article

Effect of Positive Bias and Pressure on Plasma Flow Characteristics in a Chemical Vapor Deposition Chamber

Bisheng Wang, Di Yang, Ximing Zhu, Yang Zhao, Shuai Wang, Jiaqi Zhu and Ming Zhai *

Harbin Institute of Technology, Harbin 150001, China
* Correspondence: zhaiming@hit.edu.cn

Abstract: To better understand how positive bias and deposition pressure affect the plasma flow properties in the deposition chamber during the bias-enhanced MPCVD process, a two-dimensional axisymmetric model based on the discharge mechanism of pure H_2 was constructed. The coupling process between different physical field models of the electromagnetic field, plasma, and temperature field in the MPCVD reactor is realized. We studied the influence of positive bias voltage and deposition pressure variation on microwave plasma flow characteristics in the deposition chamber. There was a bias voltage threshold phenomenon in the case of positive bias, and the suitable value range was narrow. Additionally, with the increase in the deposition pressure, the electron temperature in the deposition chamber tends to increase locally and reaches its maximum value when the pressure is approximately 30 torr. It provides new ideas and guidance for optimizing the process parameter setting of the bias-enhanced MPCVD process.

Keywords: positive bias voltage; plasma flow characteristics; chemical vapor deposition; multiphysics

check for updates

Citation: Wang, B.; Yang, D.; Zhu, X.; Zhao, Y.; Wang, S.; Zhu, J.; Zhai, M. Effect of Positive Bias and Pressure on Plasma Flow Characteristics in a Chemical Vapor Deposition Chamber. *Processes* **2022**, *10*, 2665. https://doi.org/10.3390/pr10122665

Academic Editors: Albert Ratner, Cherng-Yuan Lin and Jiaqiang E

Received: 17 August 2022
Accepted: 5 December 2022
Published: 11 December 2022

Publisher's Note: MDPI stays neutral with regard to jurisdictional claims in published maps and institutional affiliations.

Copyright: © 2022 by the authors. Licensee MDPI, Basel, Switzerland. This article is an open access article distributed under the terms and conditions of the Creative Commons Attribution (CC BY) license (https://creativecommons.org/licenses/by/4.0/).

1. Introduction

Microwave plasma chemical vapor deposition (MPCVD) is an emerging technology commonly used in the preparation of crystalline materials [1] and has broad application prospects in the preparation of high-quality carbon material and tool coatings [2–4]. The MPCVD process is complex and includes a variety of physical and chemical processes that vary greatly in both temporal and spatial scales. Compared with other CVD processes, MPCVD has significant advantages in synthesizing large-area diamond films [5] and has a wider range of applicable parameters, which provides the possibility for applications in various situations [6]. It can achieve low-temperature growth [7], carbon nanotube alignment growth, and structural control [8]. In depositing the carbon material with the MPCVD apparatus, a DC bias voltage can be applied between the substrate and the deposition chamber to superimpose the electrical and electromagnetic excitations.

Stöckel et al. [9,10] explored the effect of positive bias pretreatment in the MPCVD system on the growth of diamonds on the Si surface through experiments. They found that the DC and plasma shapes changed during the bias pretreatment process, as did the deposition density on the substrate, its chemical and crystalline properties, and the nucleation density of subsequent diamond growth. Based on this, a relatively complete bias model is proposed. Chiang et al. [11] found that applying positive substrate bias also enhanced diamond nucleation on the surface of smooth Si substrates. The nucleation density could be increased to 10^{10} cm^{-2}, generating more uniformly textured diamond films at lower microwave power and deposition pressure. The positive bias-enhanced CVD process has greater advantages in preparing high-quality diamond films.

Thus far, there are very few numerical simulation studies on the bias-enhanced MPCVD process in the literature, and most are experimental studies on the process, which mainly focus on the process parameters affecting the surface quality and growth rate of the deposited carbon materials. However, studies on how the positive bias voltage affects the plasma flow characteristics in the deposition chamber are rare.

The numerical model of the MPCVD process was first established by German scientists Füner et al. [12,13], who developed a computational model for simulating the electromagnetic field and plasma density distribution in the MPCVD reaction chamber. Japanese scholars Yamada et al. [14,15] proposed a calculation method based on a fluid model that calculated parameters such as the electromagnetic field distribution and electron number density in the deposition cavity by coupling Maxwell's equations and the fluid conservation equation of electrons. The energy conservation equation of the electron temperature distribution is obtained. Then, Yamada et al. [16,17] introduced the gas composition based on the plasma model and first calculated the power density of the plasma according to the coupling of the electron transport equation and Maxwell's equation, then used this as the heat source term to solve the governing equation of the gas species distribution. This method has since been optimized to simulate the more complex CH4 discharge reaction mechanism [18] and other gas components (Ar [19] and N2 [16]).

In this paper, plasma is regarded as a special fluid, and by studying its macroscopic performance, it has a certain guiding significance for the parameter control of practical engineering applications.

'Plasma flow characteristics' are the plasma macroscopic flow field properties defined by imitating the general fluid. The change of the flow field in the deposition chamber is observed by increasing the bias strength to provide a reference for engineering applications, so the difference between electron flow and ion flow is not specifically shown. This paper uses the multiphysics simulation software COMSOL Multiphysics 6.0 to establish a two-dimensional axisymmetric plasma model of pure H_2 discharge. Version 6.0 of the COMSOL Multiphysics® software is released by COMSOL in Sweden. According to the established multiphysics coupling model, the influence of different positive bias intensities on the plasma flow characteristics in the deposition chamber is calculated. The influence of the intensity change of positive bias voltage and deposition pressure on plasma flow characteristics was explored, and its mechanism of action in the chemical vapor deposition process was analyzed.

2. Materials and Methods

The MPCVD equipment model studied in this paper is the SEKI AX5200S made in Seki Technotron Corp. from Japan, which belongs to the quartz plate microwave plasma resonator type. It is often used to prepare diamond films. The microwave source provides a 2.45 GHz microwave, and the volume fraction of H_2 in the input gas is generally above 90%. The schematic diagram of the specific device is shown in Figure 1.

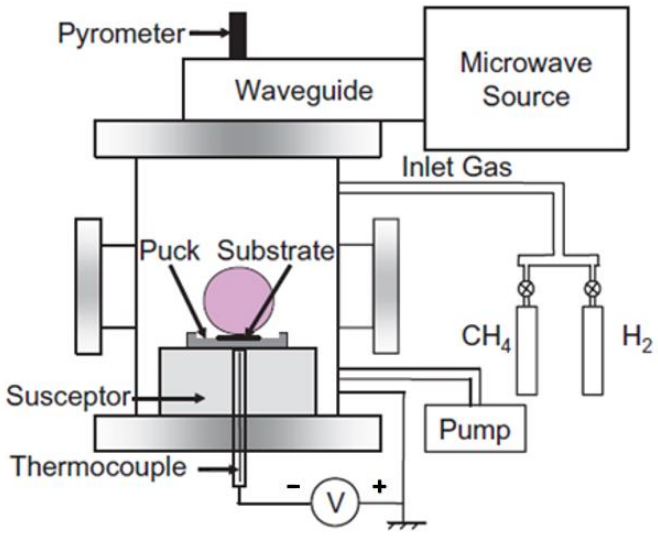

Figure 1. Schematic diagram of microwave plasma chemical vapor deposition device [20].

In solving the model, it is necessary first to calculate the electric field distribution, then calculate the electromagnetic field, that is, to solve Maxwell's equations. Equation (1) can be obtained by solving Maxwell's equations:

$$\nabla \times (\frac{1}{\mu_r}(\nabla \times \vec{E})) - k_0^2(\varepsilon_r - \frac{i\sigma}{\omega\varepsilon_0})\vec{E} = 0 \quad (1)$$

where, w is the angular frequency of the electromagnetic wave, ε_r and μ_r are the relative permittivity and relative permeability, respectively.

Plasma is equivalent to a dielectric in the electromagnetic field, so its conductivity and permittivity should be considered when calculating the electromagnetic field distribution, both of which can be represented by the following equations [21]:

$$\sigma_p = \frac{\omega_p^2 \varepsilon_0 v_m}{(\omega^2 + v_m^2)} \quad (2)$$

$$\varepsilon_p = 1 - \frac{\omega_p^2}{(\omega^2 + v_m^2)} \quad (3)$$

where, ω_P and v_m are the plasma's angular and effective collision frequencies, respectively.

The plasma is calculated by the method of drift-diffusion approximation. In the solution process, the shape of the plasma is assumed to be stable, and the following formula provides its governing equation:

$$\frac{\partial n}{\partial t} + \nabla \cdot \left(n\vec{u}\right) = R_n \quad (4)$$

$$mn\left[\frac{\partial \vec{u}}{\partial t} + \left(\vec{u} \cdot \nabla\right)\vec{u}\right] = qn\left(\vec{E} + \vec{u} \times \vec{B}\right) - \nabla \cdot p + \dot{R_d} \quad (5)$$

$$\frac{\partial}{\partial t}\left(\frac{3}{2}p\right) + \nabla \cdot \frac{3}{2}\left(p\vec{u}\right) + p\nabla \cdot \vec{u} + \nabla \cdot \vec{q} = R_\varepsilon \quad (6)$$

where, R_n is the particle number variable in the collision process, R_d is the particle momentum variable in the collision process, $R\varepsilon$ is the energy density variable in the collision process, n is the particle number density, $\vec{u}$ represents the average velocity of the particle, and $\vec{q}$ is the heat flux vector.

The electron collision reaction rate is calculated from the collision cross-section:

$$r_e = \gamma \int \varepsilon\sigma(\varepsilon) f(\varepsilon) d\varepsilon \cdot X_i N_n n_e \quad (7)$$

where, r_e is the reaction rate of the electron production and consumption, γ is the square root of twice the electron charge mass ratio, σ is the electron impact cross section, f is the electron energy distribution function, X_i is the mass fraction of the ith component, N_n is the number density of heavy particles, n_e is the number density of electrons.

In calculating the heat transfer model, the convection effect can be ignored due to the low gas flow in the deposition chamber. The governing equation for the heat transfer model calculation is:

$$\nabla\left(k\nabla T_g\right) + Q_{gas} = 0 \quad (8)$$

$$Q_{gas} = \frac{3}{2}\delta n_e v_m k_B \left(T_e[K] - T_g[K]\right) \quad (9)$$

where, k is the thermal conductivity of the gas; Q_{gas} is the heat source term due to the collision between electrons and neutral gas molecules; δ is the energy loss coefficient of the collision between electrons and neutral gas molecules; k_B is the Boltzmann constant.

Mesh generation is a key step in model calculation. A proper mesh generation method can consider both computational efficiency and accuracy. The mesh generation function of

the COMSOL Multiphysics 6.0 software is used. Considering the simulation complexity, different mesh precisions are selected for different calculation domains. The upper part of the calculation domain is only used for simple electromagnetic field calculations, so the region meshes with coarse elements. The region contains 490 mesh elements with a minimum mass of 0.5561 and an average of 0.8108. The lower part of the computational domain needs more sophisticated multi-physical field coupling calculations, so more refined mesh settings are required. The figure of meshing can be seen in Figure 2.

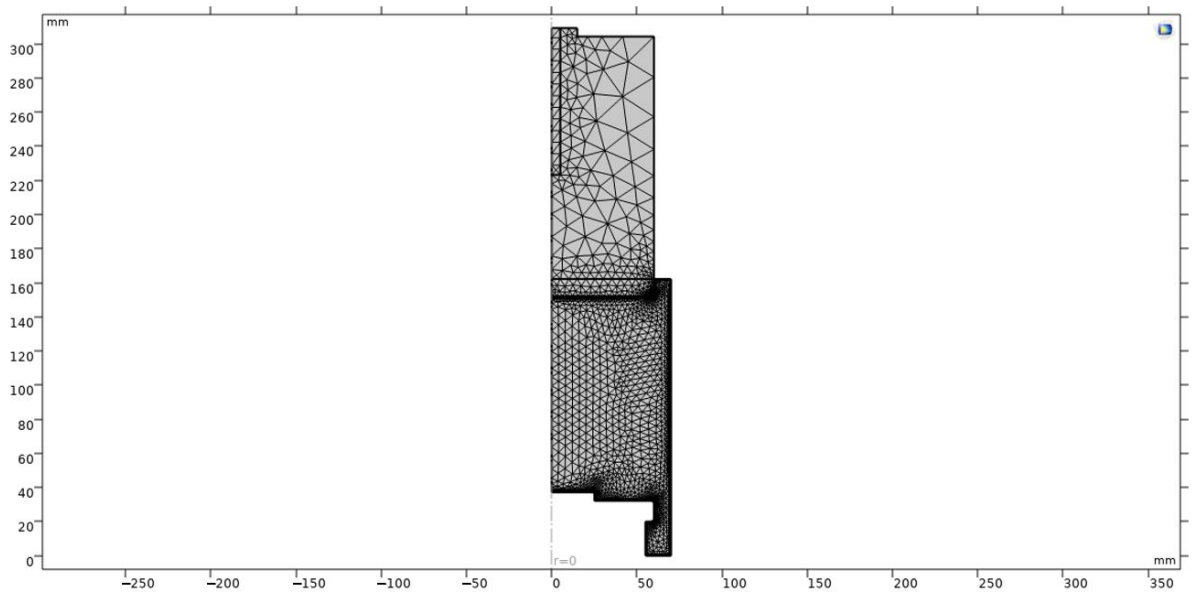

Figure 2. Mesh generation.

The relationship between the bias current and the intensity on the substrate surface was selected to verify the rationality and credibility of the physics coupling model. The results are shown in Figure 3.

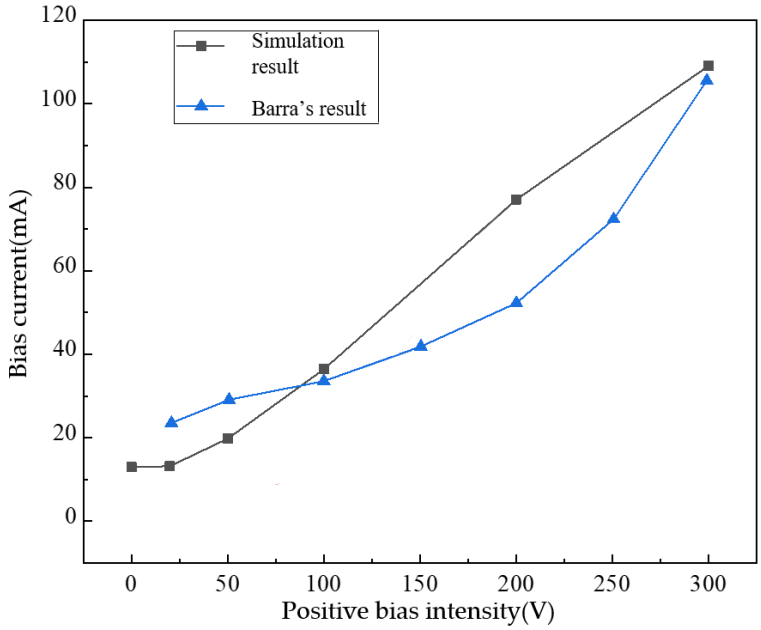

Figure 3. Variation of bias current with bias intensity.

In the process of synthesizing diamond by MPCVD equipment, Barrat [22] measured the variation of the bias current on the substrate surface with the negative bias intensity

of the substrate when the pressure was 10 torr, and the microwave power was 600 W, as shown in the blue curve in the figure shown. The qualitative law shown by the curve formed by the data is consistent. As the bias strength increases, the bias current also increases. Although there are numerical errors, they are enough to prove the rationality and credibility of the multiphysics coupling model.

3. Results

3.1. Effect of Positive Bias on Plasma Flow Characteristics

When a positive bias is applied to the substrate, the increased bias strength will influence the plasma flow characteristics. Figure 4 shows the contours of the velocity distribution in the deposition chamber under four working conditions. The contours under the four working conditions of 0, +100, +200, and +300 V were compared and analyzed. In this simulation, the deposition pressure is 10 torr, and the microwave power is selected at 600 W.

Under the condition that the deposition pressure remains unchanged, the distribution of the velocity field in the chamber does not change greatly when the strength of the positive bias is changed. However, the maximum velocity value in the chamber increases with bias strength. When the bias voltage changes from 0 to +100 V, the maximum speed increases by 1.55%. When the bias voltage changes from +100 to +200 V, the maximum speed increases by 1.36%, and when the bias voltage is changed from +200 V to +300 V, the maximum speed increases by 2.52%. By analyzing and comparing the above data, when the bias voltage is in the range of +100 V to +200 V, the increase in the maximum flow velocity in the chamber is relatively slow. As the positive bias strength continues to increase, the magnitude of the increase in flow velocity within the chamber is enhanced.

Figure 5 shows the contour plots of the electron temperature distribution under four different working conditions. Under the positive bias of the substrate, the narrow thermal region of the electron temperature disappears, and the high-temperature region of the electron temperature is dispersed into the deposition chamber and shows a very chaotic point-like distribution. Although it is seemingly irregular, the high-temperature regions are mainly concentrated on the sidewall of the reactor and the surface of the substrate table below the substrate, that is, the grounded surface. It is because when the substrate is in a positive bias state, the ground surface instead has a relatively low potential. As a result, an ion sheath forms on the ground surface, creating a region of high electron temperature. Under positive bias, electrons and ions move in different directions. Due to the difference between the properties of electrons and ions, the surrounding electric field has changed greatly, so the phenomenon of abnormally high field strength occurs. It is a kind of edge effect.

The electron temperature in the deposition cavity shows this distribution because the substrate bias voltage generates a high field strength area through the edge effect (shown in Figure 6) and then transfers the energy to the electrons near the surface. Moreover, because the electron density in the peripheral area of the deposition cavity is low, the collision effect is weakened, the electron energy loss is reduced, and the energy carried by free electrons is increased. The macroscopic performance is that the electron temperature is increased. However, this distribution of high-energy free electrons will cause most of the input energy to be dissipated on the reactor wall. It cannot be transferred to neutral particles or positive ions, thus affecting the deposition process and energy utilization rate.

In addition, the electron density distribution shown in Figure 7 can more intuitively observe the flow direction of particles in the deposition chamber during the deposition process.

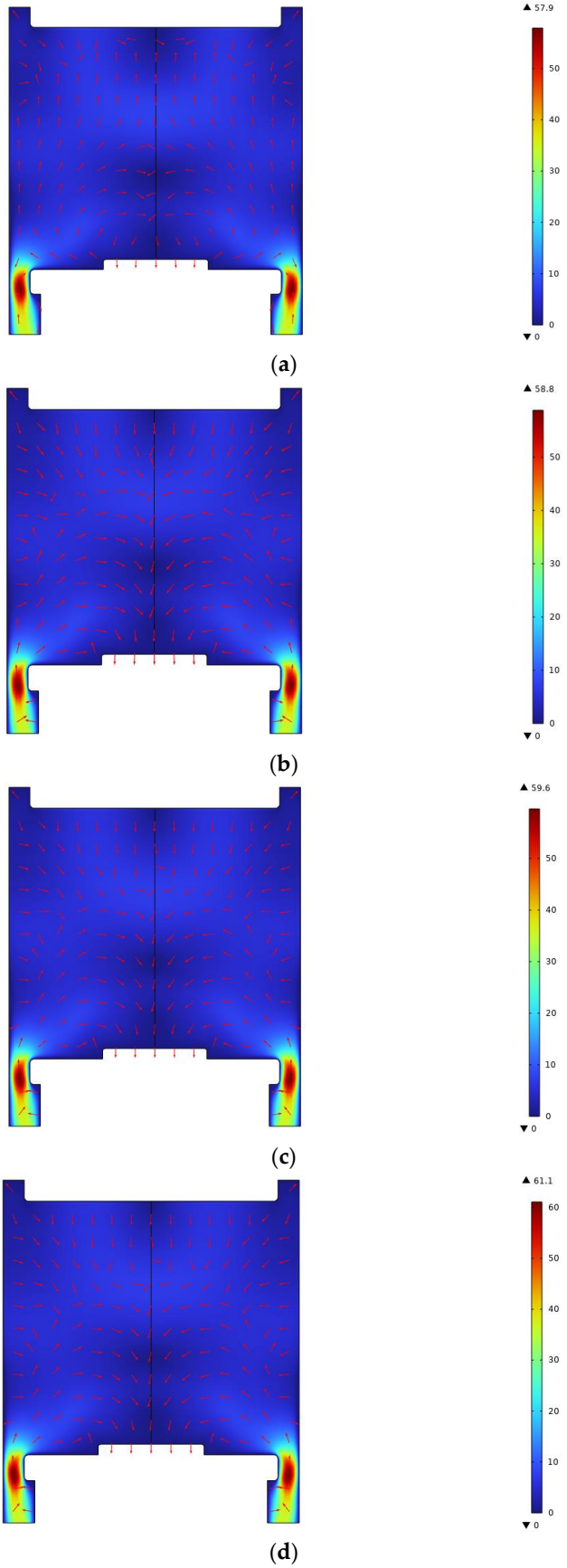

Figure 4. Contours of velocity distribution in the deposition chamber (m/s). (**a**) 0 V; (**b**) +100 V; (**c**) +200 V; and (**d**) +300 V.

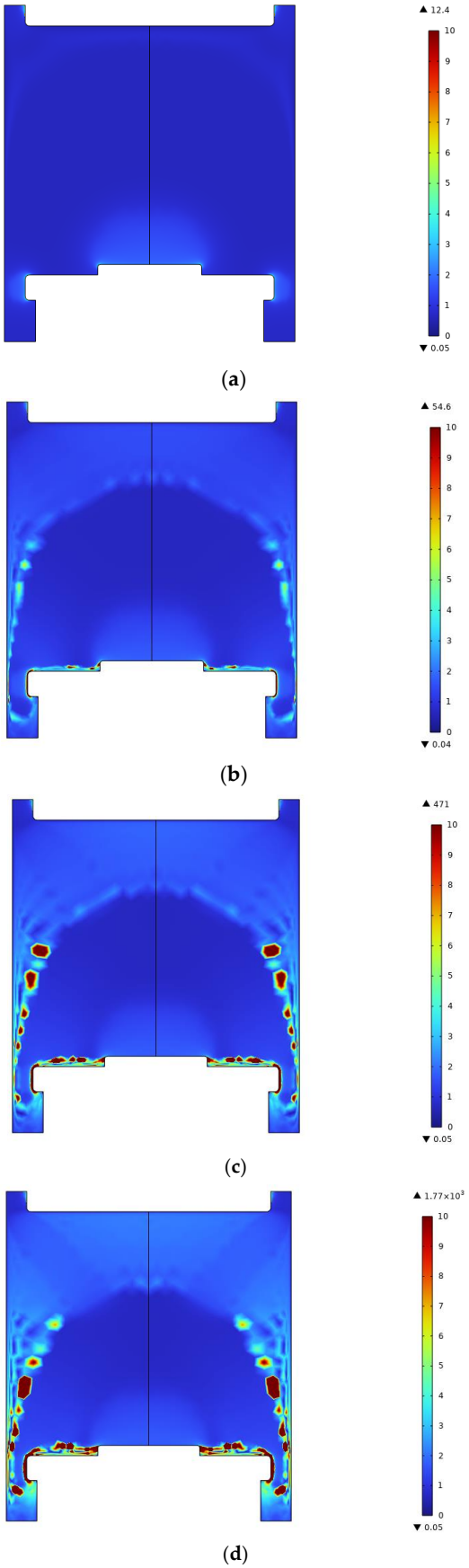

Figure 5. Contour plots of electron temperature distribution in the deposition chamber (eV). (**a**) 0 V; (**b**) +100 V; (**c**) +200 V; and (**d**) +300 V.

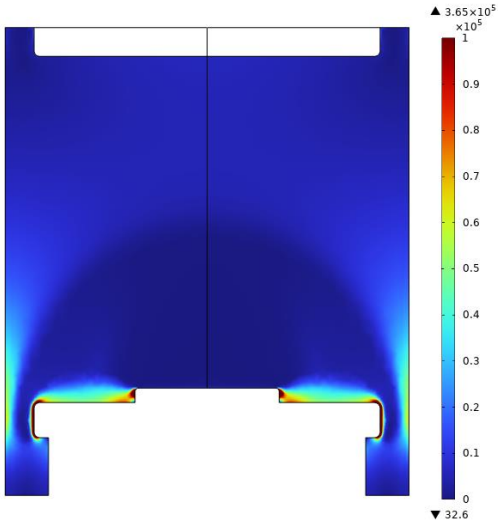

Figure 6. Contour plot of electron field distribution in the deposition chamber (V/m).

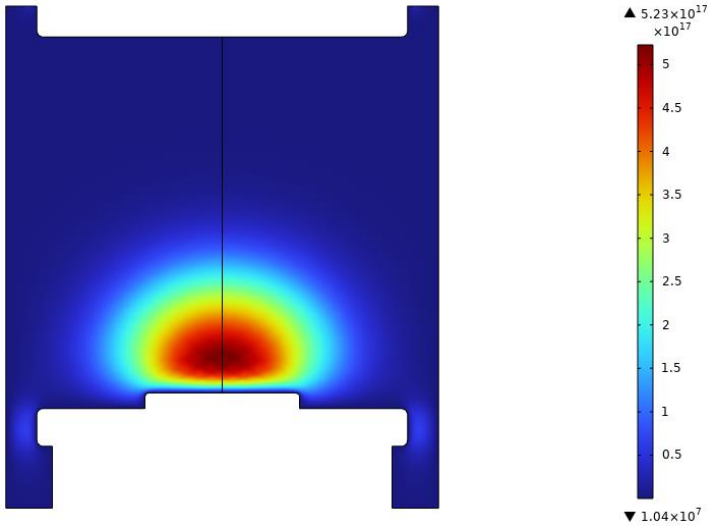

(**a**)

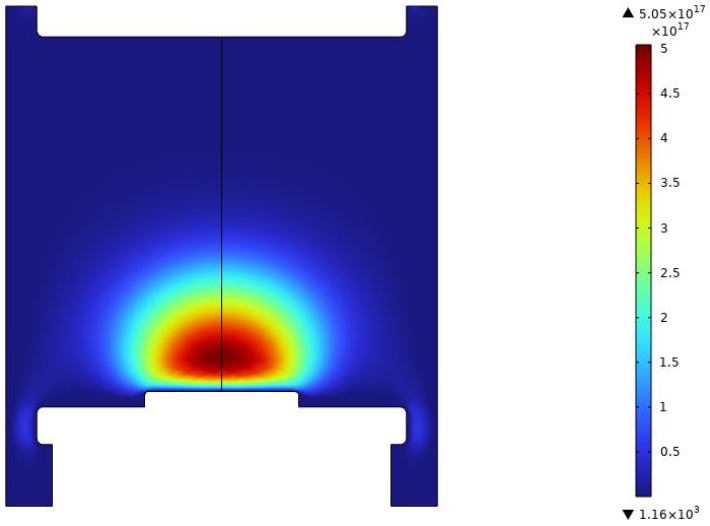

(**b**)

Figure 7. *Cont.*

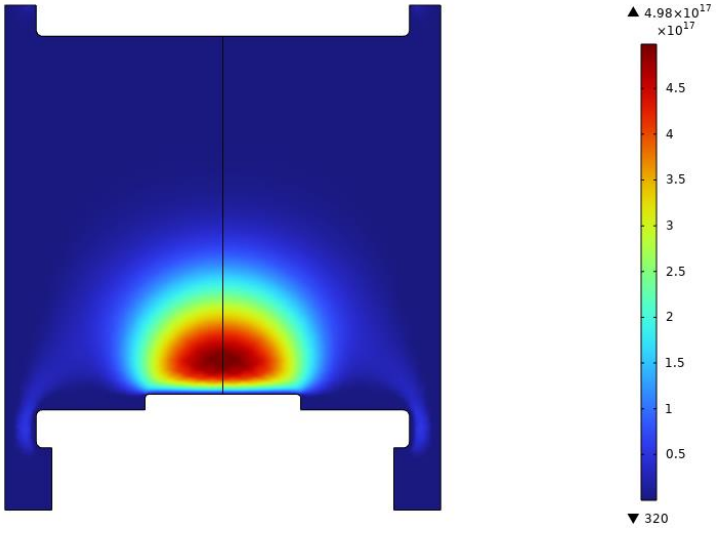

(**c**)

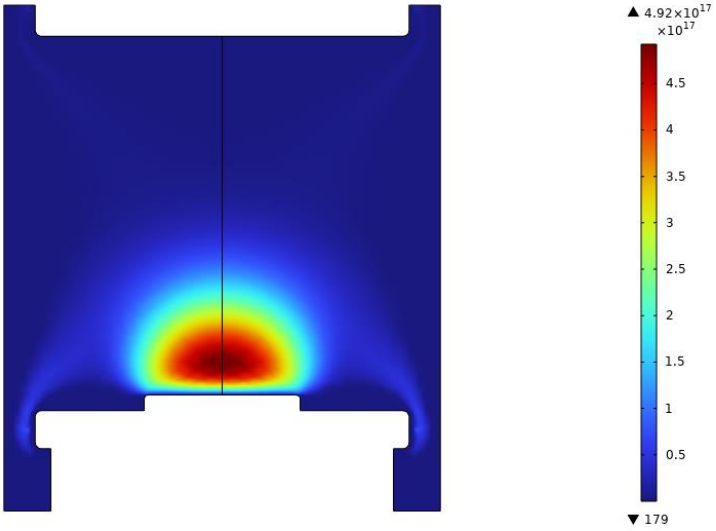

(**d**)

Figure 7. Contour plots of electron density distribution in the deposition chamber ($1/m^3$). (**a**) 0 V; (**b**) +100 V; (**c**) +200 V; and (**d**) +300 V.

Figure 8 shows the variation law of the axial electron average temperature in the deposition chamber with the bias strength of the substrate. The changing trend of electron temperature is consistent, which generally decreases first and then increases. The electron temperature is relatively stable in the central area of the substrate and gradually increases in the edge area of the substrate. Applying a positive bias voltage will make the distribution of high-energy free electrons in the deposition chamber more dispersed, thereby affecting the plasma flow characteristics in the chamber.

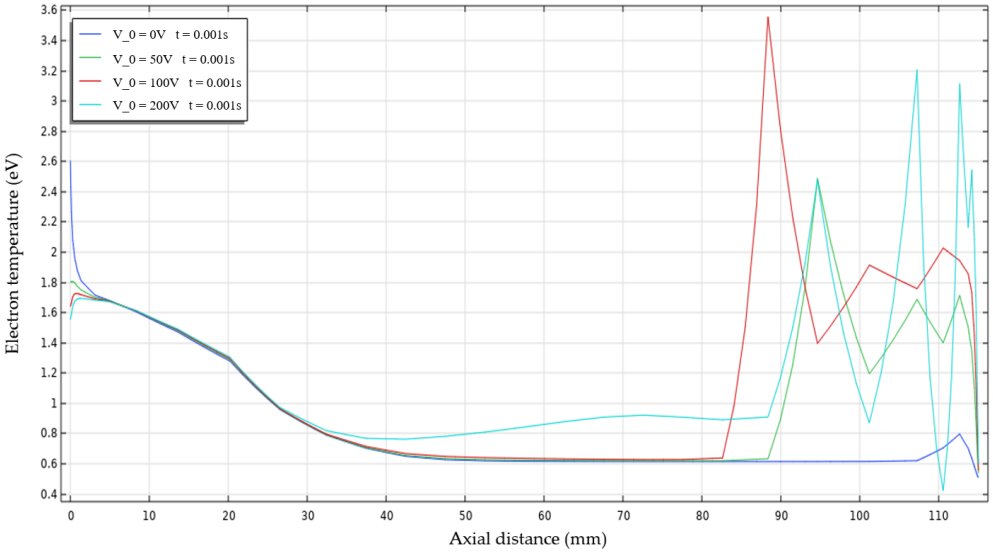

Figure 8. Axial Electron average temperature.

3.2. Effect of Deposition Pressure on Plasma Flow Characteristics

The collision process shown in Table 1 is considered. Although it is a rather simplified H_2 discharge mechanism, which includes the main reactions that generate H atoms, H_2^+ ions and excited H_2.

Table 1. The collision process involved.

Reaction	Equation	Collision Type	Δε (eV)
1	$e + H_2 \rightarrow 2e + H_2^+$	ionization	15.4
2	$e + H_2 \rightarrow e + H_2^*$	excitation	15.0
3	$e + H_2 \rightarrow e + H + H$	dissociation	8.9
4	e + H => 2e + H^+	ionization	13.6
5	H + H => H_2	association	−8.9
6	e + H => H* + e	excitation	10.2

The calculation conditions selected in this paper are 10, 30, 50, and 70 torr. In the simulation, the bias voltage is 0 V, and the microwave power is selected at 600 W. The first three reactions in Table 1 are mainly considered when analyzing the influence of air pressure.

The variation of the velocity distribution inside the deposition chamber is shown in Figure 9. A relatively obvious hemispherical velocity field is formed above the substrate with the increase in deposition pressure. At the same time, the velocity change at the exit of the chamber gradually becomes gentle. When the deposition pressure changed from 10 to 30 torr, the maximum flow velocity in the chamber decreased by 27.72%. When the deposition pressure changed from 30 to 50 torr, the maximum flow velocity in the chamber decreased by 8.99%. When the deposition pressure changed from 50 to 70 torr, the maximum flow velocity in the chamber decreased by 2.33%. By analyzing and comparing the above data, the increase in the deposition pressure decreases the maximum flow velocity in the chamber. With the increase in deposition pressure, the velocity field at the place where the plasma ball is formed above the substrate changes obviously. Therefore, it is speculated that the increase in the deposition pressure has a certain enhancement effect on the plasma flow.

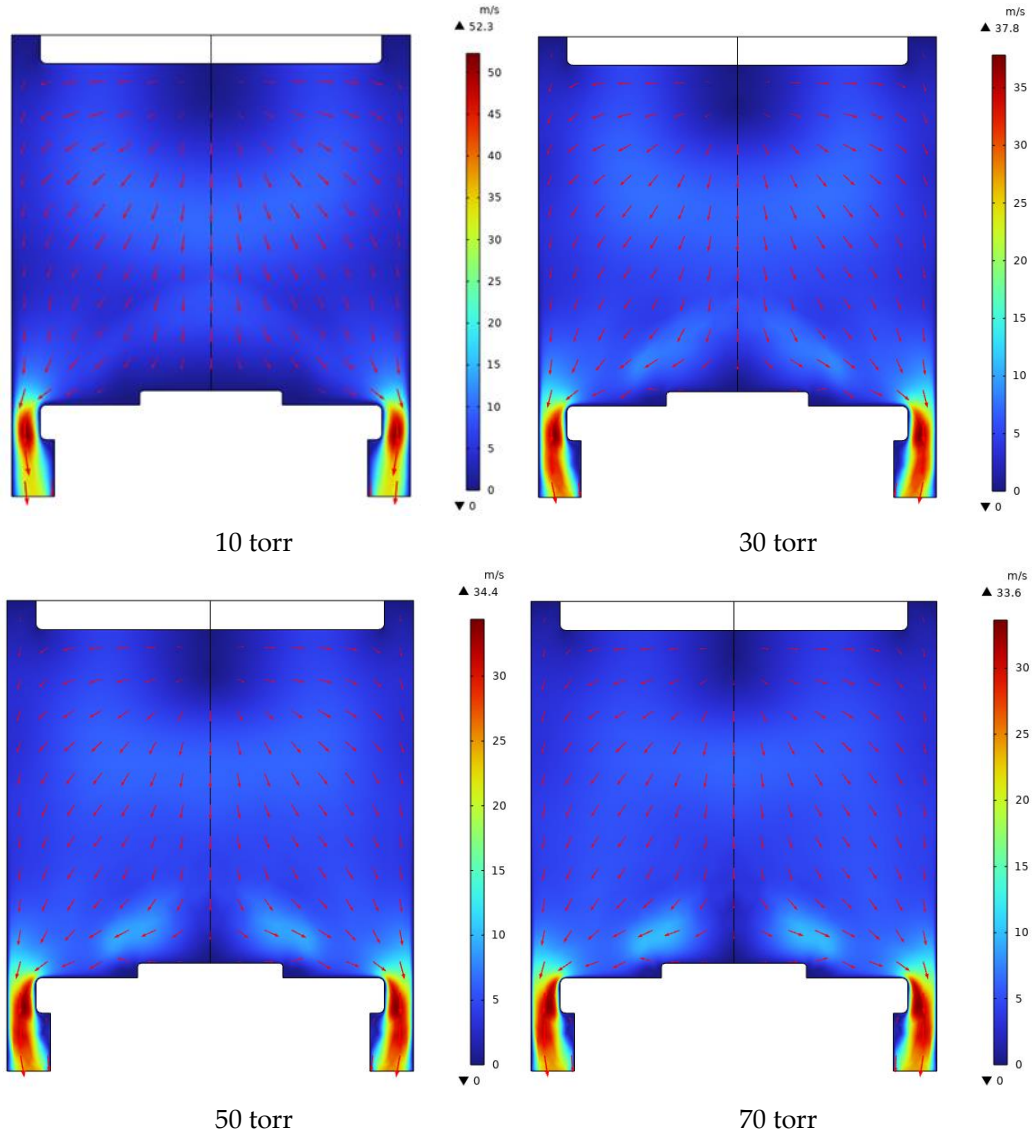

Figure 9. Contour plots of velocity distribution in the deposition chamber (m/s).

The variation in the temperature distribution inside the deposition chamber is shown in Figure 10. With the increase in deposition pressure, the temperature field above the substrate gradually becomes flat, and the center of the plasma ball is the maximum temperature. When the deposition pressure changed from 10 to 30 torr, the maximum temperature in the chamber increased by 9.55%. When the deposition pressure changed from 30 to 50 torr, the maximum temperature in the chamber decreased by 5.81%. When the deposition pressure changed from 50 to 70 torr, the maximum temperature in the chamber decreased by 6.17%. By analyzing and comparing the data above, the maximum temperature value in the chamber first increases and then decreases with the increase in deposition pressure. From the change in the temperature field distribution in the cloud map, the increase in deposition pressure gradually shrinks the high-temperature area in the chamber. The temperature at the center of the plasma ball will reach a maximum when the deposition pressure is approximately 30 torr.

The rear part of the curves in Figure 11 shows the opposite trend compared to the front. With increasing pressure, the electron temperature of the substrate increases too. Although the pressure causes the collision effect to increase, the electron density also decreases simultaneously. The probability of collision between the electron and other

particles decreases, causing a small increase in the electron temperature, which then affects the temperature field distribution in the chamber.

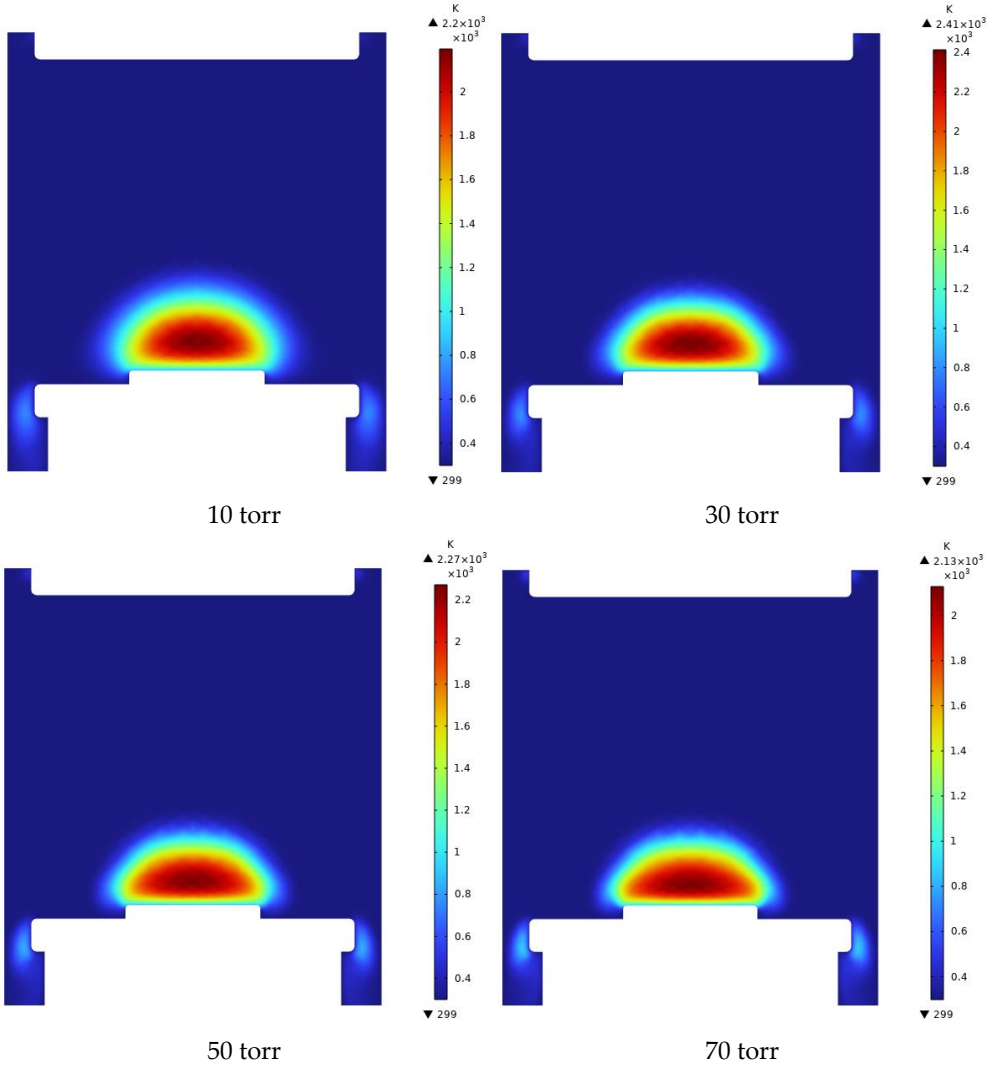

Figure 10. Contour plots of temperature distribution in the deposition chamber (K).

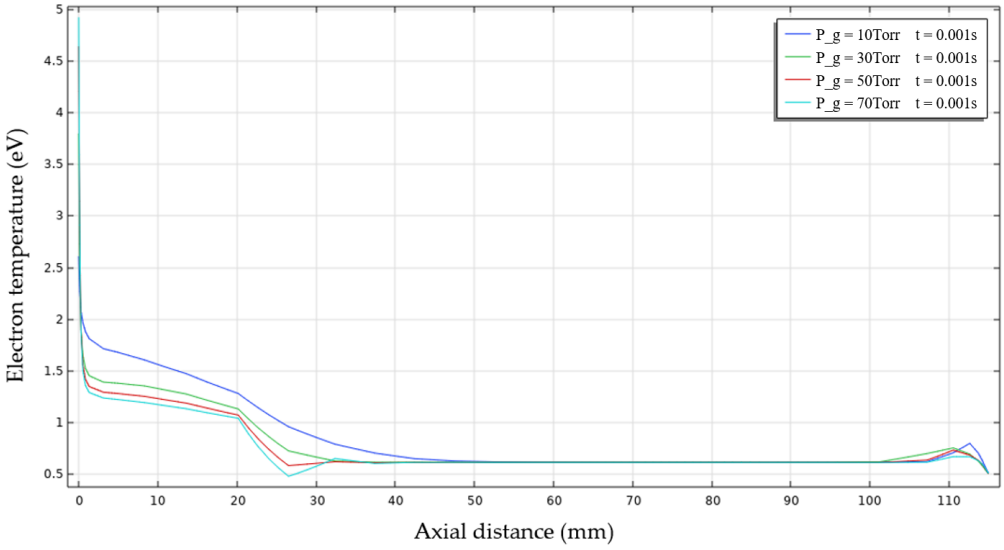

Figure 11. Axial electron temperature distribution in the deposition chamber.

4. Discussion

Under the positive bias of the substrate, the narrow thermal region of the electron temperature disappears, and the high-temperature region of the electron temperature is dispersed into the deposition chamber and presents a very chaotic point-like distribution. Although it seems irregular, the high-temperature regions are mainly concentrated on the side walls of the reactor and the surface of the substrate table below the substrate, that is, the grounded surface. It is because when the substrate is in a forward-biased state, the ground surface instead has a relatively low potential, so an ion sheath is formed on the ground surface, resulting in a region of high electron temperature.

With the increase in bias intensity, the increase rate of the average electron temperature in the deposition chamber decreases, while the increase rate of the maximum electron temperature increases and decreases. The result is opposite to that in the case of negative bias. The distribution of high-energy free electrons in the deposition chamber tends to be more dispersed, adversely affecting the deposition process.

The pressure affects the plasma characteristics within the deposition chamber by changing the mean free path between electrons and other particles. Under low-pressure conditions, the free travel of electrons is greater, the collision probability is lower, and the plasma volume is larger.

With the increase in deposition pressure, the free path of electrons decreases, the collision effect increases, the electron density also decreases, and the decrease in electron density reduces the collision probability. Therefore, the negative correlation between electron density and collision probability results in a small increase in the plasma deposition area under high-pressure conditions.

5. Conclusions

In summary, under the positive bias condition, it can be found that when the bias voltage is in the range of +100 V to +200 V, the increase in the maximum flow velocity in the chamber is relatively slow. As the positive bias strength continues to increase, the magnitude of the increase in flow velocity within the chamber is enhanced. Applying a positive bias voltage will make the distribution of high-energy free electrons in the deposition chamber more dispersed, thereby affecting the particle motion in the chamber.

When the microwave power remains unchanged and the deposition pressure changes, the effect on the plasma properties in the deposition chamber is achieved by changing the mean free path between electrons and other particles. With the increase in pressure, the electron temperature in the deposition chamber increases locally and reaches the maximum value of approximately 30 torrs. It is the decrease in electron density and the increase in collision probability occurring simultaneously owing to the change in pressure.

Author Contributions: Conceptualization, B.W. and D.Y.; methodology, X.Z. and B.W.; software, Y.Z. and S.W.; validation, X.Z. and M.Z.; investigation, M.Z. and B.W.; resources, X.Z., J.Z. and M.Z.; writing—original draft preparation, B.W. and D.Y.; writing—review and editing, X.Z. and M.Z. All authors have read and agreed to the published version of the manuscript.

Funding: This research received no external funding.

Conflicts of Interest: The authors declare no conflict of interest.

References

1. Zhi, T.; Tao, T.; Liu, B.; Wang, X.; Hu, W.; Chen, K.; Xie, Z.; Zhang, R. High quality CVD single crystal diamonds grown on nanorods patterned diamond seed. *Diam. Relat. Mater.* **2021**, *119*, 108605. [CrossRef]
2. Li, G.; Yin, S.; Tan, C.; Chen, L.; Yu, M.; Li, L.; Yan, F. Fast Photothermoelectric Response in CVD-Grown PdSe2 Photodetectors with In-Plane Anisotropy. *Adv. Funct. Mater.* **2021**, *31*, 2104787. [CrossRef]
3. Li, S.; Wang, J.; Zhu, Z.; Liu, D.; Li, W.; Sui, G.; Park, C.B. CVD carbon-coated carbonized loofah sponge loaded with a directionally arrayed MXene aerogel for electromagnetic interference shielding. *J. Mater. Chem. A* **2021**, *9*, 358–370. [CrossRef]
4. Chen, Z.; Lian, Y.Y.; Liu, X.; Feng, F.; Yan, B.-Y.; Wang, J.-B.; Lv, Y.-W.; Song, J.-P.; Liu, C.-J.; Cai, L.-Z. Recent research and development of thick CVD tungsten coatings for fusion application. *Tungsten* **2020**, *2*, 83–93. [CrossRef]

5. Weng, J.; Liu, F.; Xiong, L.W.; Wang, J.; Sun, Q. Deposition of large area uniform diamond films by microwave plasma CVD. *Vacuum* **2018**, *147*, 134–142. [CrossRef]
6. Liu, Y.; He, J.; Zhang, N.; Zhou, Y.; Huang, K. Advances of microwave plasma-enhanced chemical vapor deposition in fabrication of carbon nanotubes: A review. *J. Mater. Sci.* **2021**, *56*, 12559–12583. [CrossRef]
7. Amama, P.B.; Ogebule, O.; Maschmann, M.R.; Sands, T.D.; Fisher, T.S. Dendrimer-assisted low-temperature growth of carbon nanotubes by plasma-enhanced chemical vapor deposition. *Chem. Commun.* **2006**, *27*, 2899–2901. [CrossRef] [PubMed]
8. Amama, P.B.; Maschmann, M.R.; Fisher, T.S.; Sands, T.D. Dendrimer-templated Fe nanoparticles for the growth of single-wall carbon nanotubes by plasma-enhanced CVD. *J. Phys. Chem. B* **2006**, *110*, 10636–10644. [CrossRef] [PubMed]
9. Sto, R.; Janischowsky, K.; Rohmfeld, S.; Ristein, J.; Hundhausen, M.; Ley, L. Diamond growth during bias pre-treatment in the microwave CVD of diamond. *Diam. Relat. Mater.* **1996**, *5*, 321–325.
10. Stöckel, R.; Janischowsky, K.; Rohmfeld, S.; Ristein, J.; Hundhausen, M.; Ley, L. Growth of diamond on silicon during the bias pretreatment in chemical vapor deposition of polycrystalline diamond films. *J. Appl. Phys.* **1996**, *79*, 768–775. [CrossRef]
11. Chiang, M.J.; Hon, M.H. Enhanced nucleation of diamond films assisted by positive dc bias. *Thin Solid Film.* **2001**, *389*, 68–74. [CrossRef]
12. Füner, M.; Wild, C.; Koidl, P. Numerical simulations of microwave plasma reactors for diamond CVD. *Surf. Coat. Technol.* **1995**, *74*, 221–226. [CrossRef]
13. Füner, M.; Wild, C.; Koidl, P. Simulation and development of optimized microwave plasma reactors for diamond deposition. *Surf. Coat. Technol.* **1999**, *116*, 853–862. [CrossRef]
14. Yamada, H.; Chayahara, A.; Mokuno, Y. Simplified description of microwave plasma discharge for chemical vapor deposition of diamond. *J. Appl. Phys.* **2007**, *101*, 063302. [CrossRef]
15. Yamada, H.; Chayahara, A.; Mokuno, Y.; Soda, Y.; Horino, Y.; Fujimori, N. Modeling and numerical analyses of microwave plasmas for optimizations of a reactor design and its operating conditions. *Diam. Relat. Mater.* **2005**, *14*, 1776–1779. [CrossRef]
16. Yamada, H. Numerical simulations to study growth of single-crystal diamond by using microwave plasma chemical vapor deposition with reactive (H, C, N) species. *Jpn. J. Appl. Phys.* **2012**, *51*, 090105. [CrossRef]
17. Yamada, H.; Chayahara, A.; Mokuno, Y.; Shikata, S.-i. Model of reactive microwave plasma discharge for growth of single-crystal diamond. *Jpn. J. Appl. Phys.* **2011**, *50*, 01AB02. [CrossRef]
18. Yamada, H.; Chayahara, A.; Mokuno, Y.; Shikata, S. Numerical microwave plasma discharge study for the growth of large single-crystal diamond. *Diam. Relat. Mater.* **2015**, *54*, 9–14. [CrossRef]
19. Yamada, H.; Chayahara, A.; Mokuno, Y. Effect of Ar addition on uniformity of diamond growth by using microwave plasma chemical vapor deposition. *Diam. Relat. Mater.* **2018**, *87*, 143–148. [CrossRef]
20. Maschmann, M.; Fisher, T.; Amama, P. Enhanced Control of Single-Walled Carbon Nanotube Properties Using MPCVD with DC Electrical Bias. In *Electronic Properties of Carbon Nanotubes*; IntechOpen: London, UK, 2011.
21. Shivkumar, G.; Tholeti, S.S.; Alrefae, M.A.; Fisher, T.S.; Alexeenko, A.A. Analysis of hydrogen plasma in a microwave plasma chemical vapor deposition reactor. *J. Appl. Phys.* **2016**, *119*, 113301. [CrossRef]
22. Barrat, S.; Saada, S.; Dieguez, I.; Bauer-Grosse, E. Diamond deposition by chemical vapor deposition process: Study of the bias enhanced nucleation step. *J. Appl. Phys.* **1998**, *84*, 1870–1880. [CrossRef]